



AALBORG UNIVERSITY
DENMARK

Aalborg Universitet

Statistical Investigation of the User Effects on Mobile Terminal Antennas for 5G Applications

Syrytsin, Igor A.; Zhang, Shuai; Pedersen, Gert F.; Zhao, Kun; Thomas, Bolin; Ying, Zhinong

Published in:
I E E Transactions on Antennas and Propagation

DOI (link to publication from Publisher):
[10.1109/TAP.2017.2681701](https://doi.org/10.1109/TAP.2017.2681701)

Publication date:
2017

Document Version
Accepted author manuscript, peer reviewed version

[Link to publication from Aalborg University](#)

Citation for published version (APA):
Syrytsin, I. A., Zhang, S., Pedersen, G. F., Zhao, K., Thomas, B., & Ying, Z. (2017). Statistical Investigation of the User Effects on Mobile Terminal Antennas for 5G Applications. *I E E Transactions on Antennas and Propagation*, 65(12), 6596 - 6605. <https://doi.org/10.1109/TAP.2017.2681701>

General rights

Copyright and moral rights for the publications made accessible in the public portal are retained by the authors and/or other copyright owners and it is a condition of accessing publications that users recognise and abide by the legal requirements associated with these rights.

- Users may download and print one copy of any publication from the public portal for the purpose of private study or research.
- You may not further distribute the material or use it for any profit-making activity or commercial gain
- You may freely distribute the URL identifying the publication in the public portal -

Take down policy

If you believe that this document breaches copyright please contact us at vbn@aub.aau.dk providing details, and we will remove access to the work immediately and investigate your claim.

Statistical Investigation of the User Effects on Mobile Terminal Antennas for 5G Applications

Igor Syrytsin, Shuai Zhang, Gert Frølund Pedersen, *Senior Member, IEEE*, Kun Zhao, Thomas Bolin, Zhinong Ying, *Senior Member, IEEE*

Abstract—In this paper the user effects on mobile terminal antennas at 28 GHz are statistically investigated with the parameters of body loss, coverage efficiency and power in the shadow. The data are obtained from the measurements of 12 users in data and talk modes, with the antenna placed on the top and bottom of the chassis. In the measurements, the users hold the phone naturally. The radiation patterns and shadowing regions are also studied. It is found that a significant amount of power can propagate into the shadow of the user by creeping waves and diffractions. A new metric is defined to characterize this phenomenon. A mean body loss of 3.2-4 dB is expected in talk mode, which is also similar to the data mode with the bottom antenna. A body loss of 1 dB is expected in data mode with the top antenna location. The variation of the body loss between the users at 28 GHz is less than 2 dB, which is much smaller than that of the conventional cellular bands below 3 GHz. The coverage efficiency is significantly reduced in talk mode, but only slightly affected in data mode.

Index Terms—user effects, antennas, mobile handset, radiation patterns, body loss, coverage efficiency, 5G applications.

I. INTRODUCTION

RECENTLY communications at the millimeter wave frequencies have become more relevant, because of the design considerations for the upcoming 5G communication systems [1]. It has been considered to use beamforming at both the base and mobile stations to overcome the path loss at the high frequencies, as described in [2]. The 28 GHz band is one of the candidate bands for the upcoming 5G communication systems.

Different phased antenna array systems have already been designed to operate at this frequency in [3], [4]. An antenna for the next generation should be able to achieve high EIRP and at the same time high antenna coverage with low power consumption [5]. Furthermore, the user effects should not be neglected when designing an antenna for the mobile terminal [5]. Interactions between the human body and millimeter-wave devices at 60 GHz have been studied in [6]. In the [7] absorption of the millimeter waves by humans has been studied. However, for the 5G communication systems, it is interesting to study interactions between a mobile terminal antenna and a human head and hand. Early investigations

This work was supported by the InnovationsFonden project of RANGE.(Corresponding author: Shuai Zhang).

Igor Syrytsin, Shuai Zhang, and Gert Frølund Pedersen are with the Antennas, Propagation and Radio Networking section at the Department of Electronic Systems, Aalborg University, Denmark (email: {igs,sz,gfp}@es.aau.dk).

Kun Zhao is with KTH-Royal Institute of Technology, Stockholm, Sweden.

Thomas Bolin and Zhinong Ying are with the Corporate Technology Office, Sony Mobile Communication AB, Lund, Sweden.

in [8] suggested that a resonance frequency of the antenna tunes down when used by a person. Big amount of power will be lost in the human hand and head and a significant change in the shape of a radiation pattern will occur. At the frequencies from 0.5 to 3 GHz, the absorption due to the user presence has been studied in [9]. The performance of the mobile handsets has been evaluated using mean effective gain (MEG) in [10] and [11]. Absorption and mismatch losses of the four antennas at 900 and 1800 MHz has been investigated in [12]. In [13] the total and mismatch efficiency and MEG of the GSM 900 antennas have been investigated. In [14] it has been concluded that 8 to 13 persons are required to obtain a reasonable estimate of the body loss mean and variation. The effects of the human body on the total radiated power (TRP) and the radiation pattern has been studied in [15] by using phantoms and humans. The impact of the user's hand/hands on the mobile antenna performance has been studied in [16] and [17], where it has been concluded that the position and height of the antenna and position of the fingers on the mobile terminal play a major role in the mobile antenna performance. The effect of the user on the coverage and the radiation pattern of a phased antenna array has been studied in [18]. However the statistical investigation of the user impact or coverage efficiency of the mobile antenna at 28 GHz has not been done yet.

This paper will focus on the investigation of the user effects on the performance of the mobile antenna at 28 GHz by measuring the mobile device prototype. The prototype includes a battery and a screen. Body loss, coverage efficiency, and shadowing effects will be studied by measuring the antenna prototype in the anechoic chamber with a user in data and talk modes. The chosen parameters will be presented in terms of the variation and mean values of the measurements on the 12 users. A new parameter will be introduced to characterize the shadowing area, which can be used to investigate how much energy can propagate around the user by creeping waves and diffractions. The coverage efficiency of the antenna is also evaluated.

II. METHODS

A. Measurement Setup

In this paper, it has been chosen to use a prototype, provided by Sony Mobile, for all of the measurements. The front and the back views of the Sony prototype are shown in Fig. 1. The prototype has 10 antennas built in it. The 10 antennas are combined into two groups of the 5 antennas. Groups are

located on the left and the right side of the phone prototype and mirrored in respect to the center of the prototype. All of the antennas have a center frequency at 28 GHz and a -10 dB bandwidth of at least 2 GHz. A screen and a battery are included in the prototype to further investigate how the antenna will perform in the real mobile device. In this paper, only one antenna will be used throughout all of the measurements. The chosen antenna is located on the right side of the prototype, as shown in Fig. 1(a). The antenna used in the measurements consists of the multiple slots located along an edge of the ground plane with a dielectric layer as shown in Fig. 2. The antenna is configured to resonate at a chosen frequency by excitation of one of the slots by the stripline on the dielectric layer. The chosen antenna geometry and applications are described in the detail in [19].

The prototype measured in the free space is shown in Fig. 3(a). The chosen notch antenna has a broad endfire radiation pattern in the direction of z-axis, as shown in Fig. 3(b). In Fig. 3(c) the polar plot of the radiation pattern in yz-plane at the frequency of 28 GHz is shown. Furthermore, there is also a little more radiation in the $-y$ axis direction (screen direction) than in the $+y$ axis direction, where the screen can support surface waves at the chosen frequency range.

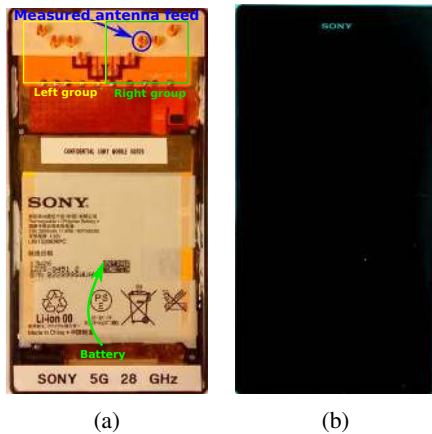


Fig. 1. Sony prototype overview: (a) back and (b) front.

For the measurements with the user a safety is added to the measurement setup, thus chosen measurement system is unable to measure 14° on the top of the coordinate system. The elevation cut of the measurement system is shown in Fig. 4. The 40° on the bottom can not be reached because of the rotating podium size limitations. The 14° on the top in θ is chosen as a starting point to be able to fix persons under test to the crane on the top with a safety rope. The “holes” in the measurement system are shown in red color and the parts where the system is able to measure are shown in green color. The “holes” will induce errors on the TRP calculation accuracy. However, those errors are acceptable, because the total area in the “holes” is much smaller than the area where the system is able to measure. From the solid angle view, the number of steradians in the holes equals to 1.6566 sr in comparison to the rest of the measurement system: $4\pi - 1.6566 = 10.9097$ sr. The solid angle in the holes is 13.13 % of the whole sphere. The solid angle of the top hole is only 0.1866 sr, which corresponds to 1.48 % of the whole

sphere. Furthermore, the antenna is oriented in such way so the strongest part of the radiation pattern is located outside of the “holes”. By doing so it has been ensured that the power missed in the holes is very small in comparison to the rest of the measured power. The rotary positioner with the chair is placed at $\theta = 180^\circ$, which will limit the amount of the energy propagating towards the bottom of the measurement setup.

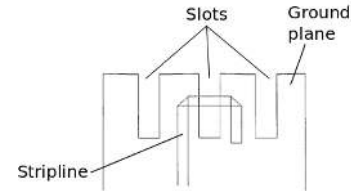


Fig. 2. Geometry of the measured antenna [19].

It has been chosen to measure the mobile prototype with the influence of a user in the four positions:

- Mobile in talk mode – antenna located on the top, as shown in Fig. 5(a).
- Mobile in talk mode – antenna located on the bottom, as shown in Fig. 5(b).
- Mobile in data mode – antenna located on the top, as shown in Fig. 5(c).
- Mobile in data mode – antenna located on the bottom, as shown in Fig. 5(d).

In all of the measurements, a user has been told to held the phone naturally. However, in the data mode, the requirement was to hold the phone horizontally and the distance between the user and the phone has been adjusted to be around 30 cm. This means that the chosen experimental setup represents the worst case scenario because the grip of the user has not been controlled. It has also been known for a long time, that a user is usually holding a phone by utilizing one of the two most common grips: firm and soft grips [12], which for the higher frequencies will introduce variation in the shadowing from the user’s hand.

B. Measures

Measures of the body loss and coverage efficiency are used in this paper to evaluate the results obtained by the measurement campaign. Furthermore, this paper will focus on investigation of the shadowing caused by the person presence in the measurement setup. The new metric of shadowing power ratio will be introduced later in the paper to describe the amount of power that has propagated around the user.

To find the body loss it is important to calculate the total radiated power of the antenna. The equation for the approximate total radiated power can be written as [9]:

$$P_{rad} = \Delta\phi\Delta\theta \sum_{\theta_{min}}^{\theta_{max}} \sum_{\phi_{min}}^{\phi_{max}} (P_V(\theta, \phi) + P_H(\theta, \phi)) \cdot \sin(\theta) \quad (1)$$

where:

- $\Delta\phi$ is a sampling step in ϕ , in the chosen setup the step equals to the 2°
- $\Delta\theta$ is a sampling step in θ , in the chosen setup the step equals to the 14°

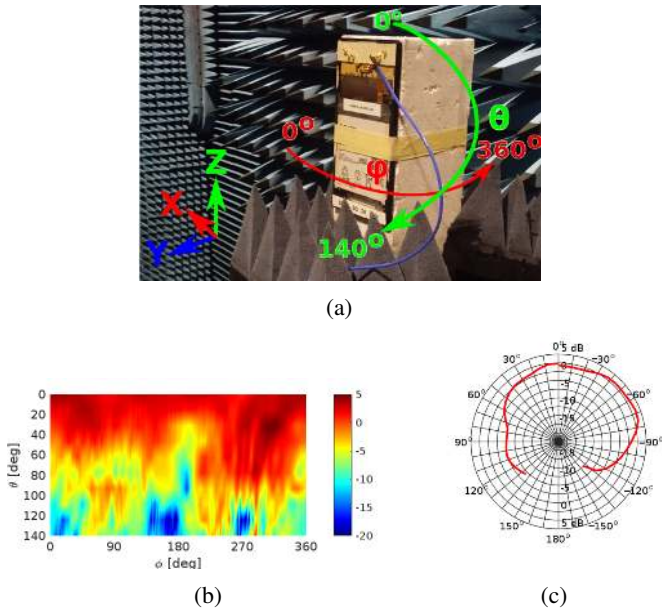


Fig. 3. (a) the picture of the prototype in free space, (b) and (c) are the radiation pattern of the chosen antenna.

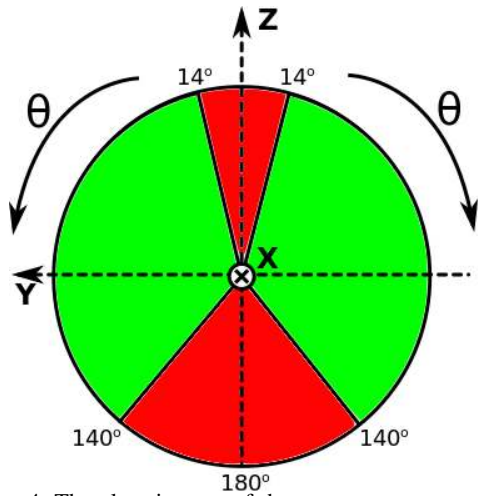


Fig. 4. The elevation cut of the measurement system.

- ϕ_{min} and ϕ_{max} are minimum and maximum angles, which are respectively defined to the 0° and 360°
- θ_{min} and θ_{max} are minimum and maximum angles, which are respectively defined to the 14° and 140°
- P_V and P_H are the power components received by the probe antenna in vertical and horizontal polarizations.

The body loss is defined in this paper as:

$$L_{body} = \frac{\eta_{free}}{\eta_{user}} \quad (2)$$

where η_{free} and η_{user} are the antenna total efficiency with and without the user.

The antenna impedance mismatch due to the user effects has been checked carefully before the measurement campaign. The reflection coefficient is always lower than -10 dB in the frequency range from 27 to 29 GHz in all the user cases. Therefore, the return loss of the cm-wave antenna is much less sensitive to the user effects than that of the low frequency antennas (< 6 GHz). The body loss at the cm-wave frequencies mainly comes from the shadowing and absorption losses

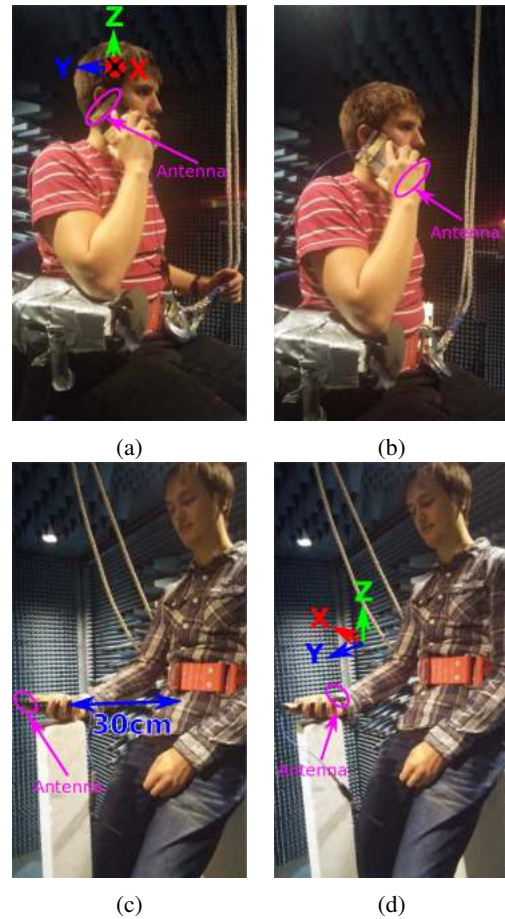


Fig. 5. The overview of the measurement setup with the user in (a) talk mode – antenna on top, (b) talk mode – antenna on bottom, (c) data mode – antenna on top, (d) data mode – antenna on bottom.

instead of antenna detuning. The mismatching losses of the antenna are neglected in this investigation.

The coverage efficiency can be defined as: [20]

$$\eta_c = \frac{\text{Coverage solid angle}}{\text{Maximum solid angle}} \quad (3)$$

where the maximum solid angle is chosen to the 4π steradians (whole space).

C. Measurement Sample

In this measurement campaign, 12 users have been measured. However, only 11 measurements has been used for the characterization of the data mode with the antenna on top of the device as the one of measurements has provided incorrect results. All of the persons in this study are males and has been chosen from the university students under 30 years old. It has been chosen to measure 12 users because, as described in [14], this number of users is enough to provide the reliable statistical data about the variation and the mean of the body loss. The histograms over the heights and weights of the users are shown in Fig. 6(a) and Fig. 6(b), respectively. It can be noticed that the relative variation in the user weight is higher than the variation the user height. A big group of the people used in the measurements is over 180 cm high.

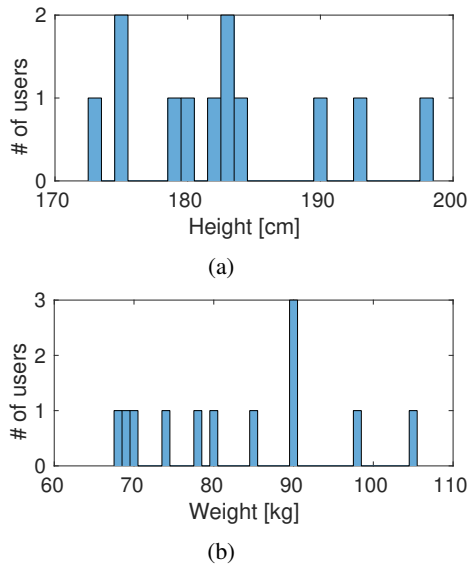


Fig. 6. The histogram of the (a) users' heights and (b) users' weights.

The photos of all the measured users in the data mode are shown in Fig. 7. The pictures give more insight on the shape of the users and gestures used.

III. EXPERIMENTAL RESULTS

In this section the results of the measurement campaign will be presented.

A. Radiation Pattern

The 3D radiation patterns of the antenna in all the four measurement setups are plotted in Fig. 8. It can be seen that the radiation patterns have similarities to the measured patterns in [18], but the position of the antenna makes a big difference on the radiation pattern shape. In the talk mode, the radiation pattern is mainly distorted by the user's head. In the data mode, the shadowing from the user's body is significant, particularly when the main beam of the antenna is pointed towards the user.

In Fig. 8(a) the radiation pattern of the antenna with the user in talk mode and the antenna located on the top is shown. The shadowing area spans 126° in θ and 150° in ϕ . The head is very close to the antenna, and thus the shadowing area is big. However, by exciting surface waves on the user's skin, the antenna can still radiate in the region from $\phi = 100^\circ$ to 190° .

In Fig. 8(b) the radiation pattern of the phone in the talk mode with the antenna on the bottom is shown. In comparison to the radiation pattern in Fig. 8(a) the pattern does not look smooth because of the waves propagating through the finger openings of the hand. The head has less impact on the antenna radiation pattern due to the larger antenna-head distance than placing the antenna on the top. Furthermore, in this position, the user's palm covers directly over the antenna. It means that there is only a small window where the antenna can radiate ($\phi = 20^\circ$ to 120°), because the user blocks the radiation pattern either by the palm or by the head. The radiation pattern is mainly supported by the scattering from the user's hand, fingers, and head.



Fig. 7. All of the measured users in the data mode.

In Fig. 8(c) the radiation pattern of the antenna on the top in data mode is shown. The main beam of the radiation pattern at $90^\circ \phi$ is pointing away from the user, and thus it is nearly not distorted by the user presence because nothing is blocking the radiation pattern in the direction of the main beam. The shadow of the standing person is very clear at $\phi = 270^\circ$.

In the last case, in Fig. 8(d), the radiation patterns of a user in the data mode with the antenna on the bottom of the prototype are shown. The radiation pattern is uneven and looks similar to the radiation pattern in Fig. 8(b). However, the person's shadow looks different from that in Fig. 8(c). It can be noticed that there is a big amount of the energy passing around the user and radiating from the back. The power radiated from the back of a person is 20 dB higher than the power in the case with antenna on the top in Fig. 8(c). The amount of the energy that is able to propagate around the user depends on the user width, height, grip type and the phone – user distance. More energy will be propagating around the user to the back if the distance is larger and the user is thinner. Here the user's body acting as a scatterer of the main beam.

In order to understand how much power has propagated around and behind the user (by creeping wave and diffraction) a new metric has been defined. The amount of the power in the shadow in comparison to the total power in whole space will be called a shadowing antenna power ratio(SAPR) in this paper.

The SAPR is defined as:

$$SAPR(\delta\theta, \delta\phi) \triangleq \frac{P_{shadow \text{ in the window}}}{P_{Total}} \quad (4)$$

$$\begin{aligned} & \Delta\phi\Delta\theta \sum_{\theta_{min}}^{\theta_{max}} \sum_{\phi_{min}}^{\phi_{max}} (P_{ant,V}(\theta, \phi) + P_{ant,H}(\theta, \phi)) \cdot \sin(\theta) \\ &= \frac{\Delta\phi\Delta\theta \sum_{14^\circ}^{140^\circ} \sum_{0^\circ}^{360^\circ} (P_{ant,V}(\theta, \phi) + P_{ant,H}(\theta, \phi)) \cdot \sin(\theta)}{\Delta\phi\Delta\theta \sum_{14^\circ}^{140^\circ} \sum_{0^\circ}^{360^\circ} (P_{ant,V}(\theta, \phi) + P_{ant,H}(\theta, \phi)) \cdot \sin(\theta)} \quad (5) \end{aligned}$$

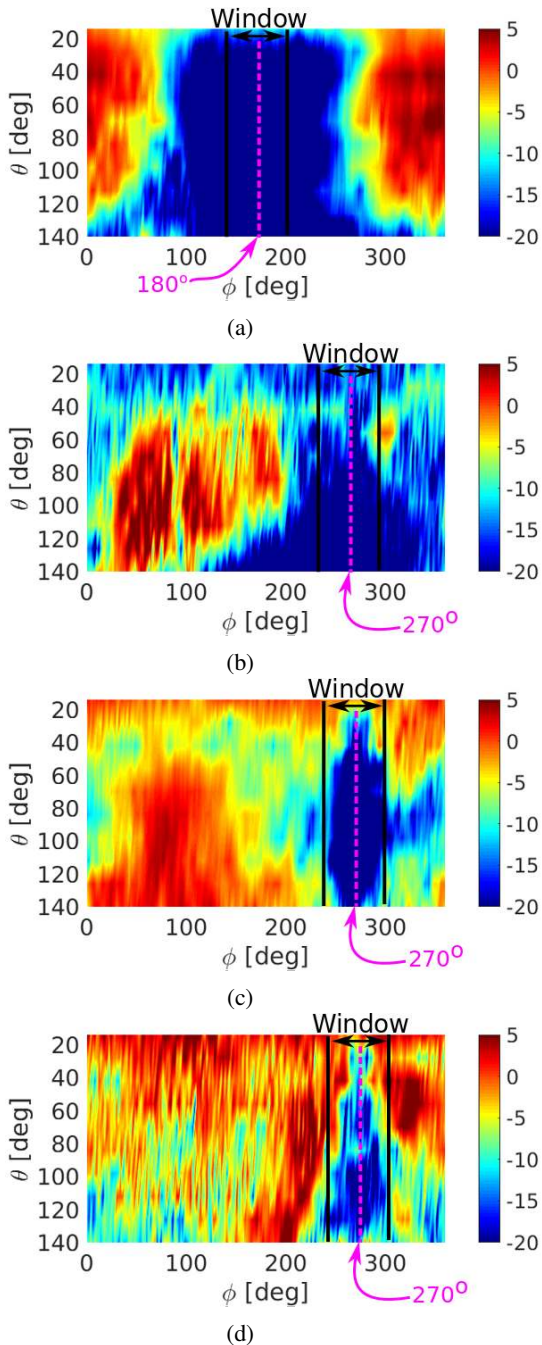


Fig. 8. The radiation pattern of the antenna with the user in (a) talk mode – antenna on top, (b) talk mode – antenna on bottom, (c) data mode – antenna on top, and (d) data mode – antenna on bottom.

where:

- $\delta\theta = \theta_{max} - \theta_{min}$ is chosen to be constant at maximum of 126° , because of the system constraints.
- $\delta\phi = \phi_{max} - \phi_{min}$ varies from 1° to 60° .
- P_{shadow} is the power in the shadow (in the chosen area of a radiation pattern).
- P_{total} is the total radiated power with the user.

The physical meaning of the formula is: how many dB in the shadow is lower than the total radiated power (TRP).

If SAPR is low then the shadowing is strong, on the other hand, if the SAPR is high then the shadowing is weak. The windows where SAPR has been calculated are displayed in

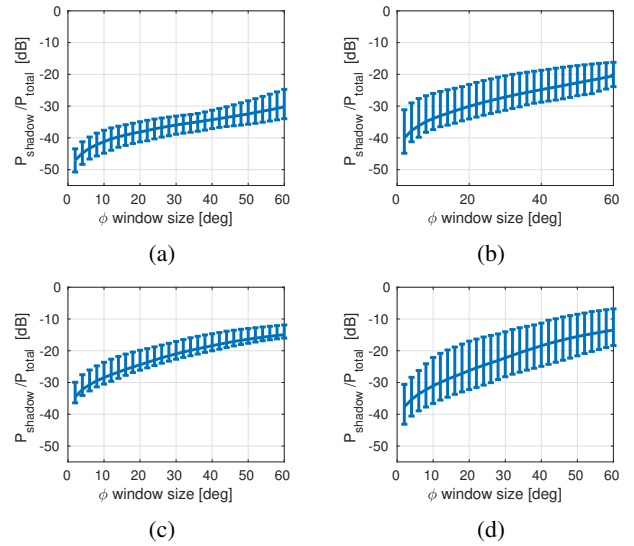


Fig. 9. SAPR of the antenna with the user in (a) talk mode – antenna on top, (b) talk mode – antenna on bottom, (c) data mode – antenna on top, and (d) data mode – antenna on bottom.

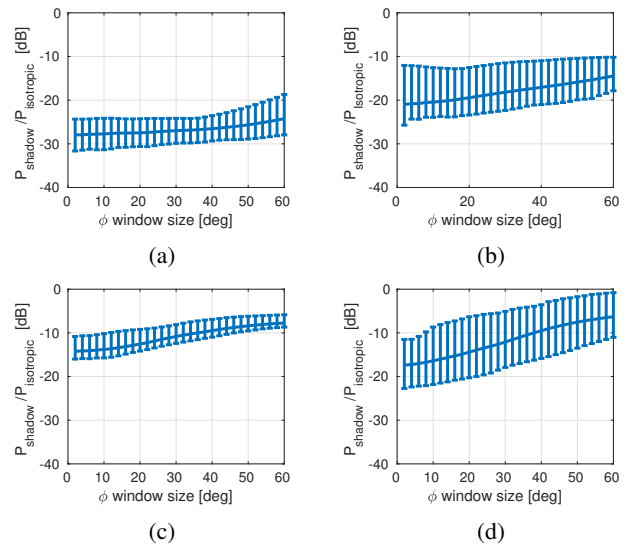


Fig. 10. SIAPR of the antenna with the user in (a) talk mode – antenna on top, (b) talk mode – antenna on bottom, (c) data mode – antenna on top, and (d) data mode – antenna on bottom.

Fig. 8. The location of the window depends on the location of the shadowing region of interest. If more power is transmitted towards the shadow the SAPR would show the amount power propagated behind the shadow by creeping waves and diffraction. The shadowing region location in this paper depends on the user and a mobile phone orientation. In Fig. 8(a) the shadow region is located at $\phi = 180^\circ$. In the rest of the sub-figures in Fig 8 the shadowing region is located at $\phi = 270^\circ$. The window length is fixed in elevation plane as $\theta = 0^\circ$ to 140° . The SAPR is calculated for the different azimuth window lengths for all of the users at 28 GHz.

An error-bar SAPR plot is displayed for the different ϕ window lengths in Fig. 9. In Fig. 9(a) the SAPR is shown for the talk mode and top antenna location. As expected, the SAPR is very low because of the big shadowing from the head. The variation in SAPR does not exceed 10 dB. The variation

is smaller for the low SAPR values. In Fig. 9(b) the SAPR for the talk mode and antenna bottom location is shown. The SAPR error-bar plot has bigger variation, especially for the small window sizes than SAPR in Fig. 9(a). Furthermore the mean SAPR curve is steeper. In Fig. 9(c) the SAPR for the data mode and antenna top location is plotted. The mean SAPR is higher than in the talk mode. The variation is on average 5-10 dB smaller than the SAPR for the talk mode. Finally, in Fig. 9(d) the SAPR for the data mode and antenna on the bottom is shown. Up to 20 dB of variation between the users can be observed.

The curves of the mean SAPR for all four setups are shown in Fig. 11. For the small window sizes, the difference in SAPR between the curves tends to decrease. The mean SAPR curve for the talk mode and top antenna location is on average 10 dB lower than the curve for the talk mode and bottom antenna location. The curves for the data mode are on average 5 dB higher than the curve for the talk mode and antenna on the bottom. It is important to address that on average the SAPR for the bottom and top antenna locations in data mode is very similar. However, the variance in SAPR for the bottom antenna location is higher. From the physical point of view, it can be explained that for the bottom antenna location sometimes a big amount of energy can propagate around the user, but on average the power in shadowing region is the same as in the case with antenna top location in data mode.

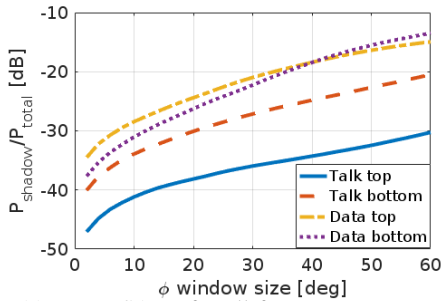


Fig. 11. Mean SAPR for all four measurement setups.

Next, the another parameter of shadow isotropic antenna power ratio (SIAPR), which is not related to antenna TRP. The SIAPR uses a dual polarized isotropic antenna as a reference (gain = 0 dB) instead of the antenna under the test itself. Where the SAPR involves the antenna radiation characteristics the SIAPR only focus on shadowing power characteristics. The SIAPR is defined as:

$$SIAPR(\delta\theta, \delta\phi) \triangleq \frac{P_{Shadow \text{ in the window}}}{P_{Isotropic \text{ antenna in the window}}} \quad (6)$$

$$\begin{aligned} & \frac{\Delta\phi\Delta\theta \sum_{\theta_{min}}^{\theta_{max}} \sum_{\phi_{min}}^{\phi_{max}} (P_{aut,V}(\theta, \phi) + P_{aut,H}(\theta, \phi)) \cdot \sin(\theta)}{\Delta\phi\Delta\theta \sum_{\theta_{min}}^{\theta_{max}} \sum_{\phi_{min}}^{\phi_{max}} (P_{iso,V}(\theta, \phi) + P_{iso,H}(\theta, \phi)) \cdot \sin(\theta)} \quad (7) \end{aligned}$$

where:

- $\delta\theta = \theta_{max} - \theta_{min}$ is chosen to be constant at maximum of 126° , because of the system constraints.
- $\delta\phi = \phi_{max} - \phi_{min}$ varies from 1° to 60° .

- P_{shadow} is the power in the shadow (in the chosen area of a radiation pattern).
- $P_{isotropic \text{ antenna}}$ is the power calculated for the same area in space for the isotropic antenna.
- $P_{aut,V}$ and $P_{aut,H}$ are vertical and horizontal power components of the antenna under the test.
- $P_{iso,V}$ and $P_{iso,H}$ are vertical and horizontal power components of the isotropic antenna.

The SIAPR for the all four test setups has been plotted in Fig.10. It can be noticed that all of the curves are flatter in respect to the curves in Fig.9, and variation between the users is more constant across the window widths. The SIAPR can be used when comparing the power in the shadowing of antennas with the different radiation patterns. In the talk mode, the different types of antennas (e.g., patch, slot, endfire-radiated notch, dipole and so on) mainly change the power distribution outside the shadow. The SIAPR is similar if different types of antennas are placed at the same location of the chassis under the same user gesture. In data mode, we choose the two cases of antenna (endfire) beam pointing at a user and pointing against a user. If the pattern is broadside, the SIAPR should be between the values of these two cases. Therefore, even though in this paper only the antenna with endfire radiation patterns are studied, the SIAPR obtained in this paper can still provide some guidance for the antenna with other radiation patterns (e.g. broadside radiation pattern).

B. Body Loss

In this section, the measured body loss will be presented. The early investigations in [8] have shown that more than 45% of the power is lost in the head and hand at the GSM and DECT frequencies. In [13] has been found that around 10.9dB of body loss is expected for the GSM frequencies. In [15] it has been found that the variation in the body loss between persons is higher when the user selected grip is used. Furthermore, a 3 dB in a standard deviation of a body loss has been observed. In [11] a body loss at the 776 MHz and 2300 MHz has been measured. The measured mean body loss has a range of 0-15 dB, of which most of the values were located under 6 dB.

The body loss has been illustrated in Fig. 12 by an error bar graph. The body loss for the measurement setup in the talk mode and the antenna located on the top of the phone is shown in Fig. 12(a). It can be observed that on average around 4 dB of the body loss is expected. However, the variations in the body loss between the users are much lower in comparison to the studies done for the lower frequency in [9] and [21] when a user selected grip is used.

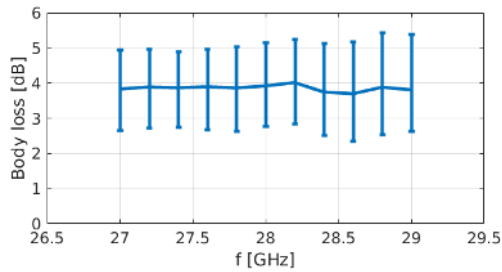
In Fig. 12(b) the body loss for the antenna on the bottom of the phone in the talk mode is displayed. From the plot, it can be noticed that the mean body loss is 0.2 to 0.3 dB lower than in Fig. 12(a), which means that there is only a small difference in the body loss when antenna located on the top or the bottom of the mobile device in the talk mode. The variation of the body loss in Fig. 12(b) is around 1 dB smaller than in Fig. 12(a).

In data mode, in Fig. 12(c) and 12(d), the variation of the body loss between the users is higher. It can be speculated that

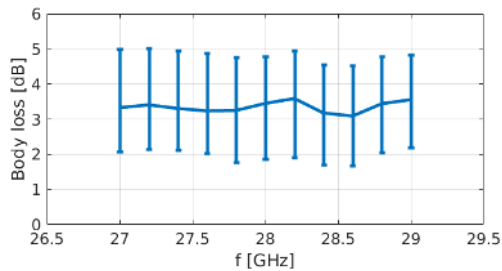
the loss is affected by the multiple variables, such as user's height, weight and grip type. If the distance between a user and a phone is not controlled then the variation between users is expected to increase dramatically because of the difference in shadowing area.

The mean body loss in the data mode and the antenna top location is very low. In Fig. 12(c) around 0.7 to 1.5 dB of the body loss is expected for this particular setup.

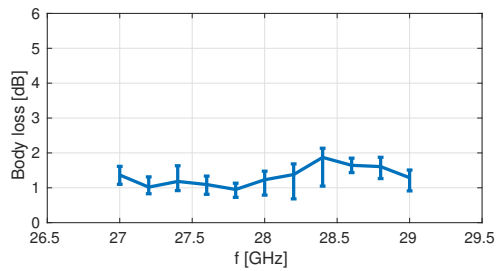
On the other hand, in the setup with the antenna located on the bottom of the mobile device in data mode the mean body loss, shown in Fig. 12(d), is comparable to the losses in the talk mode. The expected mean body loss ranges from 3.5 to 4 dB. The variance of the body loss, calculated from the



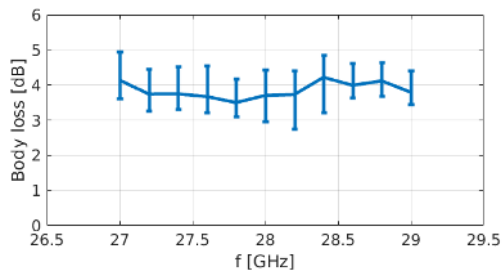
(a)



(b)



(c)



(d)

Fig. 12. The minimum, maximum and mean body loss in frequency band from 27 to 29 GHz for the users in (a) talk mode – antenna on top, (b) talk mode – antenna on bottom, (c) data mode – antenna on top, and (d) data mode – antenna on bottom.

statistical data, is shown in Fig. 13. A variance of the body loss in the talk mode and antenna on top varies from 0.4 to 0.7 dB in the measured band. The body loss in talk mode and antenna on the bottom has less variation in the band. Those two curves have same variance value at 28.7 GHz. The variance in the data mode and bottom antenna location is 0.2 to 0.5 dB lower than the variance of the body loss in the talk mode. The variance of the body loss for the setup in the data mode and antenna top location is the lowest of all four, which is under 0.1 dB.

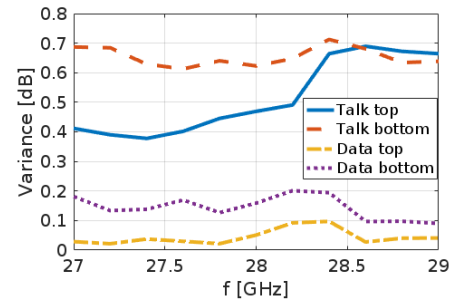


Fig. 13. Variance of the body loss for the all four setups.

C. Coverage efficiency

In this subsection the impact of the user on the antenna coverage at 28 GHz will be studied. Usually, coverage efficiency metric is used to calculate the coverage of the phased array. However, in this paper, the coverage efficiency of only one antenna element is calculated. If the element is placed into an array the antenna gain should be multiplied by the array factor. For example, for an array of 8 elements an increase of 9 dB is expected. The behavior of the antenna array can be predicted to some extent by looking on the coverage of the one element. The coverage efficiency of the antenna in all four of the case studies is plotted in Fig. 14, where the red curve represents the coverage efficiency of the antenna in the free space.

Both curves for the talk mode in Fig. 14(a) and 14(b) look very similar. The variation in the coverage for different users increases with the bottom antenna. Both curves follow the red curve only for the high and very low antenna gains.

The coverage efficiency error bar plots for the data mode are shown in Fig. 14(c) and 14(d). Both mean coverage efficiency curves have a shape very similar to the curve of the antenna coverage in the free space. However, the variance between the users is higher for the antenna located on the bottom of the mobile device in Fig. 14(d). It can be observed in both pictures that the user effects actually very close to the free space curve.

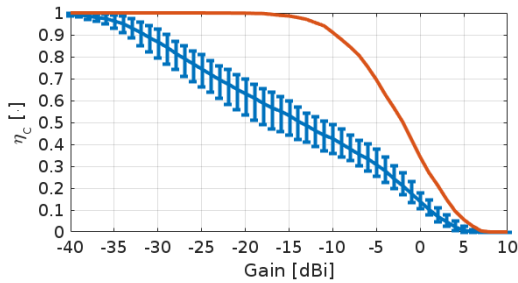
IV. COMPARISON OF THE RESULTS

The variation of the SAPR is different for each of the four measurement setups. The SAPR mean, variance, minimum and maximum measured values are shown in Tab. I for the window of 30°. This shadowing window width is encountered in all four setups.

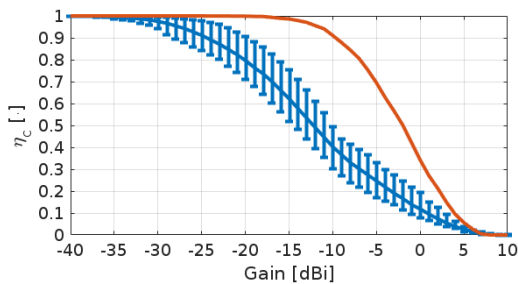
The mean body loss of at least 3.2 dB is expected in the talk mode. In data mode when the antenna is located on the bottom

Table I. Measured parameters at 28 GHz

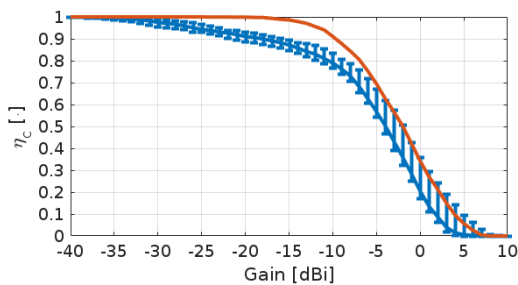
Setup	SAPR @ 30° [dB]				Body loss [dB]				Coverage efficiency @ 0 dBi			
	Mean	Var	Max	Min	Mean	Var	Max	Min	Mean	Var	Max	Min
Talk – top	-35.95	4.07	-33.13	-38.85	3.86	0.45	5.1	2.8	0.14	4.14E-4	0.18	0.1
Talk – bottom	-27.15	9.77	-20.44	-31.32	3.25	0.64	4.8	1.9	0.12	9.74E-4	0.19	0.08
Data – top	-20.98	2.60	-17.07	-22.67	1.45	0.02	1.5	0.8	0.20	0.0027	0.36	0.17
Data – bottom	-22.25	12.84	-14.03	-28.17	3.45	0.13	4.5	3	0.11	0.0025	0.26	0.07



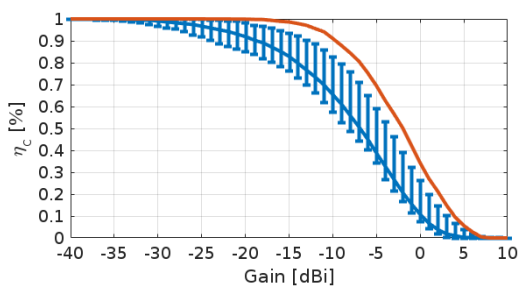
(a)



(b)



(c)



(d)

Fig. 14. The coverage efficiency of the (a) antenna on top in talk mode, (b) antenna on bottom in talk mode, (c) antenna on top in data mode, and (d) antenna on bottom in data mode. The red curve represent the coverage efficiency in the free space.

of the mobile device, a loss of 3.5-4 dB is expected. In the data mode and antenna top location, only 1 dB of the body loss is expected. The variation in the loss between the users does not exceed 2 dB. Higher body losses in data mode are expected when the distance between a user and a mobile device is smaller than the chosen 30 cm. The mean, variance, maximum and minimum values for the antenna center frequency of 28 GHz are shown in Tab. I.

The coverage efficiency of the antenna at the 0 dBi is at least 30 % lower for the antenna used in talk mode in comparison to the free space. The coverage of the antenna in the data mode is very similar to the coverage of the antenna in free space. The more detailed overview of the mean, variance, maximum and minimum values of the coverage efficiency at 0 dBi is shown in Tab. I. The realized gain of 0 dBi is chosen to show how much coverage the antenna has compared to the ideal isotropic antenna. When antennas are combined into array, a gain increase of 9 dBi over a single element is expected for the 8-element array. Thus, the coverage efficiency value at 0 dB will tell approximately how much coverage an array composed of such antenna elements would have at 9 dBi gain.

V. CONCLUSION

In this paper, a study of the body loss, shadowing area and coverage efficiency of the mobile terminal antenna at 28 GHz has been presented. The results are based on the measurement campaign involving 12 persons.

From all the studies of the multiple radiation patterns, it can be concluded that in data mode, when the beam is pointing towards the user, it is still possible to decrease the power in the shadowing region by the creeping waves and diffractions. Furthermore, when antenna located on the bottom of the mobile device the palm and the fingers of the user will affect the radiation pattern. A significant amount of power is still able to propagate through the hand. A measure of shadowing power ratio has been proposed to characterize the shadowing region. The highest mean SAPR has been obtained from the measurements in the data mode with the antenna on the bottom of a device.

The measure of SAPR has been proposed and calculated statistically from the radiation patterns in talk and data modes. For the small window sizes the biggest shadowing is expected for the talk mode with the antenna on top. The smallest variation of SAPR can be observed for the setups where the antenna was positioned on the top of the mobile device.

The mean body loss of less than 4 dB for all of the measurement setups has been observed. The body loss is much lower than the body loss observed for the low frequencies (<6 GHz). Furthermore, the variation in the body loss between the users is less than 4 dB, and even less than 1 dB in some cases.

The coverage efficiency for the antenna at 0dB gain is between 10 and 20%. The variation in the coverage efficiency of 19% in the worst case and 11% in the best case has been observed.

To make the presented study more general the measurement with the children, woman and people older than 30 could be carried out in the future. From the study, it can clearly be seen that to obtain the optimal antenna performance at least two antennas on the top and bottom should be integrated into the design of a mobile device.

ACKNOWLEDGMENT

The authors would like to thank Kristian Bank for helping with the setup of the measurement equipment. Furthermore authors would like to thank 7th and 9th semester Wireless Communication System students at the Aalborg University for the participation in the measurement campaign.

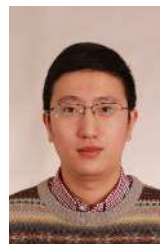
REFERENCES

- [1] T. S. Rappaport, S. Sun, R. Mayzus, H. Zhao, Y. Azar, K. Wang, G. N. Wong, J. K. Schulz, M. Samimi, and F. Gutierrez, "Millimeter wave mobile communications for 5g cellular: It will work!," *IEEE Access*, vol. 1, pp. 335–349, 2013.
- [2] W. Roh, J. Y. Seol, J. Park, B. Lee, J. Lee, Y. Kim, J. Cho, K. Cheun, and F. Aryanfar, "Millimeter-wave beamforming as an enabling technology for 5g cellular communications: theoretical feasibility and prototype results," *IEEE Communications Magazine*, vol. 52, pp. 106–113, February 2014.
- [3] N. Ojaroudiparchin, M. Shen, and G. Pedersen, "Multi-layer 5g mobile phone antenna for multi-user mimo communications," *Telecommunications Forum Telfor (TELFOR), 2015 23rd*, pp. 559–562, Nov 2015.
- [4] W. Hong, K. Baek, Y. Lee, and Y. G. Kim, "Design and analysis of a low-profile 28 ghz beam steering antenna solution for future 5g cellular applications," *Microwave Symposium (IMS), 2014 IEEE MTT-S International*, pp. 1–4, June 2014.
- [5] W. Hong, K. H. Baek, Y. Lee, Y. Kim, and S. T. Ko, "Study and prototyping of practically large-scale mmwave antenna systems for 5g cellular devices," *IEEE Communications Magazine*, vol. 52, pp. 63–69, September 2014.
- [6] T. Wu, T. S. Rappaport, and C. M. Collins, "The human body and millimeter-wave wireless communication systems: Interactions and implications," in *2015 IEEE International Conference on Communications (ICC)*, pp. 2423–2429, June 2015.
- [7] O. P. Gandhi and A. Riazi, "Absorption of millimeter waves by human beings and its biological implications," *IEEE Transactions on Microwave Theory and Techniques*, vol. 34, pp. 228–235, Feb 1986.
- [8] J. Toftgard, S. N. Hornsleth, and J. B. Andersen, "Effects on portable antennas of the presence of a person," *IEEE Transactions on Antennas and Propagation*, vol. 41, pp. 739–746, Jun 1993.
- [9] J. B. Andersen, J. O. Nielsen, and G. F. Pedersen, "Absorption related to hand-held devices in data mode," *IEEE Transactions on Electromagnetic Compatibility*, vol. 58, pp. 47–53, Feb 2016.
- [10] J. O. Nielsen and G. F. Pedersen, "Mobile handset performance evaluation using radiation pattern measurements," *IEEE Transactions on Antennas and Propagation*, vol. 54, pp. 2154–2165, July 2006.
- [11] J. O. Nielsen, B. Yanakiev, I. B. Bonev, M. Christensen, G. F. Pedersen, C. Luxey, A. Djalied, and I. Diccmm, "User influence on the mean effective gain for data mode operation of mobile handsets," in *2012 6th European Conference on Antennas and Propagation (EUCAP)*, pp. 2759–2763, March 2012.
- [12] M. Pelosi, O. Franek, M. B. Knudsen, G. F. Pedersen, and J. B. Andersen, "Antenna proximity effects for talk and data modes in mobile phones," *IEEE Antennas and Propagation Magazine*, vol. 52, pp. 15–27, June 2010.
- [13] K. R. Boyle, "The performance of gsm 900 antennas in the presence of people and phantoms," in *Antennas and Propagation, 2003. (ICAP 2003). Twelfth International Conference on (Conf. Publ. No. 491)*, vol. 1, pp. 35–38 vol.1, March 2003.

- [14] J. O. Nielsen, G. F. Pedersen, K. Olesen, and I. Z. Kovacs, "Statistics of measured body loss for mobile phones," *IEEE Transactions on Antennas and Propagation*, vol. 49, pp. 1351–1353, Sep 2001.
- [15] J. Krogerus, J. Toivanen, C. Icheln, and P. Vainikainen, "Effect of the human body on total radiated power and the 3-d radiation pattern of mobile handsets," *IEEE Transactions on Instrumentation and Measurement*, vol. 56, pp. 2375–2385, Dec 2007.
- [16] J. Ilvonen, O. Kivekas, J. Holopainen, R. Valkonen, K. Rasilainen, and P. Vainikainen, "Mobile terminal antenna performance with the user's hand: Effect of antenna dimensioning and location," *IEEE Antennas and Wireless Propagation Letters*, vol. 10, pp. 772–775, 2011.
- [17] J. Holopainen, O. Kivekas, J. Ilvonen, R. Valkonen, C. Icheln, and P. Vainikainen, "Effect of the user's hands on the operation of lower uhf-band mobile terminal antennas: Focus on digital television receiver," *IEEE Transactions on Electromagnetic Compatibility*, vol. 53, pp. 831–841, Aug 2011.
- [18] K. Zhao, J. Helander, D. Sjoberg, S. He, T. Bolin, and Z. Ying, "User body effect on phased array in user equipment for 5g mm wave communication system," *IEEE Antennas and Wireless Propagation Letters*, vol. PP, no. 99, pp. 1–1, 2016.
- [19] J. Helander and Z. Ying, "Stripline coupled antenna with periodic slots for wireless electronic devices." US Patent, US 14/534,445, May, 2016.
- [20] J. Helander, K. Zhao, Z. Ying, and D. Sjöberg, "Performance analysis of millimeter-wave phased array antennas in cellular handsets," *IEEE Antennas and Wireless Propagation Letters*, vol. 15, pp. 504–507, 2016.
- [21] J. Krogerus, J. Toivanen, C. Icheln, and P. Vainikainen, "User effect on total radiated power and 3-d radiation pattern of mobile handsets," *Antennas and Propagation, 2006. EuCAP 2006. First European Conference on*, pp. 1–6, Nov 2006.



Igor Syrytsin was born in Saratov, Russia, in 1988. He received the B.S. degree in electronic engineering and IT and M.S. degree in wireless communication systems from Aalborg University, Aalborg, Denmark, in 2014 and 2016, respectively. Currently, he is pursuing the Ph.D. degree at Department of Electronic Systems at Aalborg University. His research interests include mm-Wave mobile antenna design and interactions between user and mobile antennas.



Shuai Zhang was born in Liaoning, China, in 1983. He received the B.E. degree from the University of Electronic Science and Technology of China, Chengdu, China, in 2007 and the Ph.D. degree in electromagnetic engineering from the Royal Institute of Technology (KTH), Stockholm, Sweden, in 2013. After his Ph.D. studies, he was a Research Fellow at KTH. In April 2014, he joined Aalborg University, Denmark, where he currently works as Assistant Professor. He is also an external antenna specialist at Bang & Olufsen, Denmark. In 2010 and 2011, he

was a Visiting Researcher at Lund University, Sweden and at Sony Mobile Communications AB, Sweden, respectively. His research interests include: mobile terminal mmwave antennas, biological effects, UWB wind turbine blade deflection sensing, MIMO antenna systems, and RFID antennas.



Gert Frølund Pedersen was born in 1965. He received the B.Sc. and E.E. (Hons.) degrees in electrical engineering from the College of Technology in Dublin, Dublin Institute of Technology, Dublin, Ireland, in 1991, and the M.Sc.E.E. and Ph.D. degrees from Aalborg University, Aalborg, Denmark, in 1993 and 2003, respectively. Since 1993, he has been with Aalborg University where he is a Full Professor heading the Antenna, Propagation and Networking LAB with 36 researchers. He is also the Head of the Doctoral School on wireless

communication with some 100 Ph.D. students enrolled. His research interests include radio communication for mobile terminals especially small antennas, diversity systems, propagation, and biological effects. He has published more than 175 peer reviewed papers and holds 28 patents. He has also worked as a Consultant for developments of more than 100 antennas for mobile terminals including the first internal antenna for mobile phones in 1994 with lowest SAR, first internal triple-band antenna in 1998 with low SAR and high TRP and TIS, and lately various multiantenna systems rated as the most efficient on the market. He has worked most of the time with joint university and industry projects and have received more than 12 M\$ in direct research funding. He is currently the Project Leader of the SAFE project with a total budget of 8 M\$ investigating tunable front end including tunable antennas for the future multiband mobile phones. He has been one of the pioneers in establishing over-the-air measurement systems. The measurement technique is now well established for mobile terminals with single antennas and he was chairing the various COST groups (swg2.2 of COST 259, 273, 2100, and now ICT1004) with liaison to 3GPP for over-the-air test of MIMO terminals. He is currently involved in MIMO OTA measurement.



Kun Zhao received the B.S. degree in Communication Engineering from Beijing University of Posts and Telecommunications (BUPT), Beijing, China in 2010 and M.S. degree in Wireless Systems from Royal Institute of Technology (KTH), Stockholm, Sweden, in 2012. Currently, he is working toward the Ph. D. degree at Department of Electromagnetic Engineering, KTH. He has been a visiting researcher at the Department of Electrical and Information Technology, Lund University, Sweden, and Sony Mobile Communication AB, Sweden. His current

research interests include mmWave antenna and propagation for 5G communications, MIMO antenna systems, multiple antennas-user interactions and body centric wireless communications.



Thomas Bolin received the M.Sc. in Applied Physics and Electrical Engineering degree from Linköping University, Sweden in 1979. From 1979 to 1983 he was an RF-engineer at ITT Standard Radio & Telefon AB in Stockholm doing 1 kW HF PA design. From 1983 to 2001 he held a technical management position at Ericsson Mobile Communications in Lund Sweden doing RF and antenna product development but also OTA measurement technology development for mobile handsets. From 2001 to 2011 he held the same position within

Sony Ericsson Mobile Communications in Lund and since 2011 at Sony Mobile Communications in Lund now more devoted to antenna research and standardization. Lately he assisted in development of cm-wave antenna arrays (15-30 GHz) for 5G.



Zhinong Ying (SM'05) is a principal engineer (senior expert) of antenna technology in Network Research Lab, Research and Technology, Sony Mobile Communication AB within Sony Group, Lund, Sweden. He joined Ericsson AB in 1995. He became Senior Specialist in 1997 and Expert in 2003 in his engineer career at Ericsson, and Principal Engineer at Sony Group. His main research interests are small antennas, broad and multi-band antenna, multi-channel antenna (MIMO) system, near-field and human body effects and measurement techniques.

He has authored and co-authored over 90 papers in various of journal, conference and industry publications. He holds more than 80 patents and pending in the antenna and mobile terminal areas. He contributed a book chapter to the well known "Mobile Antenna Handbook 3rd edition" edited by Dr. H. Fujimoto. He had invented and designed various types of multi-band antennas and compact MIMO antennas for the mobile industry. One of his contributions in 1990's is the development of non-uniform helical antenna. The innovative designs are widely used in mobile terminal industry. His patented designs have reached a commercial penetration of more than several hundreds million products in worldwide. He received the Best Invention Award at Ericsson Mobile in 1996 and Key Performer Award at Sony Ericsson in 2002. He was nominated for President Award at Sony Ericsson in 2004 for his innovative contributions. He has been guest professor in Zhejiang University, China since 2002. He served as TPC Co-Chairmen in International Symposium on Antenna Technology (iWAT), 2007, and served as session organizer of several international conferences including IEEE APS, and a reviewer for several academic journals. He is a senior member of IEEE. He was a member of scientific board of ACE program (Antenna Centre of Excellent in European 6th frame) from 2004 to 2007.